Hearing Research 396 (2020) 108070

Contents lists available at ScienceDirect

Hearing Research

journal homepage: www.elsevier.com/locate/heares

Level coding by phase duration and asymmetric pulse shape reduce channel interactions in cochlear implants

Gunnar Lennart Quass[a,b,*], Peter Baumhoff[a], Dan Gnansia[c], Pierre Stahl[c], Andrej Kral[a,b]

[a] Institute for AudioNeuroTechnology (VIANNA), ENT Clinics, Hannover Medical School, 30625 Hannover, Germany
[b] Cluster of Excellence "Hearing4All" (EXC 2177)
[c] Oticon Medical, 06220 Vallauris, France

ARTICLE INFO

Article history:
Received 3 June 2020
Revised 21 August 2020
Accepted 31 August 2020
Available online 4 September 2020

Keywords:
Cochlear implants
Pulse symmetry
Loudness coding
Spread of excitation
Channel interactions

ABSTRACT

Conventional loudness coding with CIs by pulse current amplitude has a disadvantage: Increasing the stimulation current increases the spread of excitation in the auditory nerve, resulting in stronger channel interactions at high stimulation levels. These limit the number of effective information channels that a CI user can perceive. Stimulus intensity information (loudness) can alternatively be transmitted via pulse phase duration. We hypothesized that loudness coding by phase duration avoids the increase in the spread of the electric field and thus leads to less channel interactions at high stimulation levels. To avoid polarity effects, we combined this coding with pseudomonophasic stimuli. To test whether this affects the spread of excitation, 16 acutely deafened guinea pigs were implanted with CIs and neural activity from the inferior colliculus was recorded while stimulating with either biphasic, amplitude-coded pulses, or pseudomonophasic, duration- or amplitude-coded pulses. Pseudomonophasic stimuli combined with phase duration loudness coding reduced the lowest response thresholds and the spread of excitation. We investigated the channel interactions at suprathreshold levels by computing the phase-locking to a pulse train in the presence of an interacting pulse train on a different electrode on the CI. Pseudomonophasic pulses coupled with phase duration loudness coding reduced the interference by 4-5% compared to biphasic pulses, depending on the place of stimulation. This effect of pseudomonophasic stimuli was achieved with amplitude coding only in the basal cochlea, indicating a distance- or volume dependent effect. Our results show that pseudomonophasic, phase-duration-coded stimuli slightly reduce channel interactions, suggesting a potential benefit for speech understanding in humans.

1. Introduction

Despite the extensive research that has been performed on cochlear implants (CIs), the number of independent channels of information a user can profit from peaks only around six to eight (Berg et al., 2019; Fishman et al., 1997; Friesen et al., 2001) and falls short of the 20 to 24 channels that normal hearing provides (Başkent, 2006; Traunmüller, 1990; Zwicker et al., 1957; Zwicker and Fastl, 1999). This leads to spectral smearing and an increase in the number of unresolved harmonics, affecting speech and music perception (Bingabr et al., 2008; ter Keurs et al., 1992). An increase in the number of active electrodes beyond eight has only a small effect on speech understanding, indicating a physical limit for the number of independent channels of information in CIs (Berg et al., 2019; Dorman et al., 1997; Friedmann et al., 2019; Kileny et al., 1992). Channel interactions play a cardinal role in this limitation.

Several mechanisms contribute to channel interactions. When individual implant electrodes are activated, an electric field spreads throughout the conducting parts of the cochlea and thus activates a large population of spiral ganglion cells. The spread of excitation is defined as the spatial extent of the activated neuronal population by a given electric stimulus, and it represents the inverse of spectral resolution. One consequence of a large spread of excitation are channel interactions: When neighboring electrodes are activated with different stimuli in close succession, the excitation patterns in the auditory nerve significantly overlap, mixing the two streams of information. Thus, distinguishing between these stimuli becomes increasingly difficult. Previous studies have tried with partial success to reduce the channel interactions by various

* Corresponding author.
E-mail address: quass.gunnar@mh-hannover.de (G.L. Quass).

https://doi.org/10.1016/j.heares.2020.108070

means, including the addition of electrodes (Fishman et al., 1997; Friesen et al., 2001), using focused stimulation like multipolar or phased array stimulation to shape the electric field (Bierer, 2007; Bierer and Middlebrooks, 2002; Kral et al., 1998; van den Honert and Kelsall, 2007), or exploring the effects of the anodic/cathodic current distribution of the stimulating pulse, referred to as pulse symmetry (Carlyon et al., 2017; Undurraga et al., 2012; van Wieringen et al., 2008). Despite these efforts, channel interactions remain an unresolved problem of CIs.

At low stimulus levels, the spread of excitation is small and channel interaction effects may manifest only weakly; however, they can increase as the amplitude is increased (Boulet et al., 2016; Pfingst et al., 1999). This effect, while also present in normal hearing, is particularly large with cochlear implants. While in most CIs, increasing loudness is coded by increasing current amplitude, there are other means to invoking a louder percept. For single pulses, the neuronal threshold and the percept of loudness are proportional to the integrated charge over time (Chatterjee et al., 2000; Parkins and Colombo, 1987; Pfingst et al., 1991). For pulse trains, an increase of pulse rate can lead to a variety of effects that influence thresholds and loudness growth (Azadpour et al., 2018; Boulet et al., 2016; Zhou et al., 2012). Thus, loudness can alternatively be coded by pulse rate or phase duration (Shannon, 1985). Increasing the pulse rate to increase loudness has been effective at lower stimulation rates in humans (McKay and McDermott, 1998), but accompanied by changes in perceptual qualities like pitch and timbre (Busby and Clark, 1997). Furthermore, without significant modification of the standard continuous interleaved sampling strategy, the stimulation rate can only be set for the entire array simultaneously. Of these two, especially increased phase duration could therefore represent an approach to code intensity without increasing the spread of excitation. This type of coding, which could be set per individual electrode, would further help to prevent reaching the compliance voltage limits of the implant even at electrodes with high threshold levels. Experimental evidence for benefits of this type of coding in terms of the spread of excitation, however, has not yet been provided.

A confounding factor is the use of biphasic pulses (BP). Biphasic pulses consist of two equal phases with reversed polarity that may be separated by a very short interphase gap. While providing charge balance, the cathodic and the anodic phase likely activate different compartments of neurons, depending on their orientation and location. Since anodic stimulation is assumed to more effectively stimulate cell bodies rather than peripheral processes, and since the spatial profile of the electric field can lead to “anodal surround” and “virtual electrode” effects in the activating function, anodic and cathodic stimuli are potentially activating slightly different, albeit largely overlapping, populations of neurons (Ranck, 1975; Rattay, 1986). Indeed, the polarity of a stimulating pulse affects the neural response: electrically evoked brainstem response thresholds and loudness perception differ between cathodic and anodic CI stimulation, with anodic pulses requiring less current than cathodic pulses to be perceived equally loud by humans (Jahn and Arenberg, 2019a; Undurraga et al., 2013). A recent modeling study suggests that this effect is likely mediated by the degeneration of peripheral processes and changes in myelination (Resnick et al., 2018). To eliminate the effect of changing polarity in the present study, we used cathodic-leading, pseudomonophasic pulses (PS) with one supra- (cathodic), and one sub-threshold (anodic) phase. Cathodic-leading PS were chosen since they have a positive effect on the compound action potential- and auditory nerve thresholds of cats and guinea pigs (Miller et al., 2001; Shepherd and Javel, 1999). Macherey et al. (2006, 2008, 2010) have demonstrated that forward masking thresholds in humans were dependent on the masker polarity and the place of the electrode in a wide bipolar configuration, indicating that the use of PS might increase the spectral resolution of CI stimulation. However, direct experimental evidence for this conclusion is missing.

In the present study we investigated whether a pseudomonophasic stimulus coupled with phase-duration-based intensity coding reduces channel interactions at high suprathreshold levels. For this, neural activity from the inferior colliculus (IC) was recorded during CI stimulation of acutely deafened and implanted guinea pigs, comparing current amplitude coding and phase duration coding of loudness, as well as biphasic and pseudomonophasic pulse shapes.

2. Materials & methods

2.1. Animal handling and anesthesia

All procedures were approved by the local state authorities (Lower Saxony state office for consumer protection and food safety, LAVES approval No. 18/2844) and were carried out in accordance with the guidelines of the European Community for the care and use of laboratory animals (EU VD 86/609/EEC) and the German Animal Welfare Act (TierSchG). A total of 16 Dunkin Hartley white guinea pigs (*Cavia porcellus*) of either sex with a minimum weight of 325 g were used in this study (6 males, 10 females). Before the experiment, all animals received a perorally applied pre-medication treatment of 0.5 g Bene-Bac® (Dechra Veterinary Products Deutschland GmbH, Aulendorf, GER) and 0.3 mg diazepam (Ratiopharm GmbH, Ulm, GER). Animals were initially anesthetized by subcutaneous injection of a mixture of 50 mg/kg Ketamine (10 %, WDT, Garbsen, GER), 10 mg/kg Xylazine (Medistar, Ascheberg, GER), and 0.1 mg/kg Atropine (B.Braun. Melsungen, GER). Analgesia was provided by subcutaneous injection of 0.05 ml Carprofen (Rimadyl, Pfizer Deutschland GmbH, Berlin, GER). All animals were then placed on a heating pad controlled by a rectal probe, received a tracheotomy, were artificially ventilated, and anesthesia was maintained on a surgical level by volatile application of isoflurane (0.5–1.7%, Baxter, Unterschleißheim, GER). The anesthesia level was controlled by adjusting the amount of isoflurane, the breathing rate, and the tidal volume. During the experiment, heart rate, end-tidal CO_2, and temperature (set to 37.7 °C) were continuously monitored, and the animals received a subcutaneous infusion of 2 ml/h Ringer’s solution.

2.2. Surgical procedure

Animals were head-fixed in a stereotaxic frame by affixing a metal bar to the head with dental cement (Paladur, Heraeus Kulzer GmbH, Hanau, GER). To access the cochlea, an incision was made above the bulla, and the skin and muscle tissues were ablated, before perforating the bulla with an injection needle and further opening it with a micro-rongeur. The cochlea was first left intact during the subsequent parietal skull surgery. To access the IC, a 0.7 cm diameter parietal trephination was made, centered around stereotaxic coordinates (Bregma + 1.25 cm AP, - 0.45 cm ML) over the left hemisphere, and a 2 × 16 channels standard NeuroNexus array was inserted at an angle of 30° – 45° (NeuroNexus Technologies, Ann Arbor, MI). The cortex was covered with silicone oil to prevent it from drying out. The electrode was advanced 3.4 – 5 mm deep into the brain until physiological pure-tone responses confirmed placement of at least one electrode shank within the central IC (see “Acoustic Stimulation”). Electrode placement was considered correct when a frequency-tuning profile was clearly visible from low frequencies to high frequencies along the electrode (Fig. 2e). After acoustic measurements were completed and with the IC electrode in place, a cochleostomy was performed by carefully drilling an opening of 0.7 mm diameter into the scala tympani of the basal turn. Subsequently, the animal was pharmacolog-

ically deafened by intracochlear application of 10% neomycin for 15 – 30 min. The neomycin was washed out by slow intrascalar instillation of Ringer's solution. After deafness was confirmed via auditory brainstem measurements (see "ABR Recordings"), a CI (Oticon medical, Smørum, DEN) with a length of 7 mm and 6 electrode contacts spaced at 1 mm center-to-center distance was implanted into the scala tympani. The return electrode was a silver ball electrode placed under the muscle tissue in the scruff. The CI and the return electrode were fixed to the animal using a tissue adhesive (Histoacryl, B.Braun, Melsungen, GER) to prevent dislocation. Upon completion of the experiment, animals received a lethal intracardiac injection of pentobarbital (Release, WDT, Garbsen, GER). The brain and the implanted cochlea were extracted and fixed in 4% PFA for subsequent histological analysis.

2.3. ABR recordings

To confirm normal hearing for each animal prior to the experiment, auditory brainstem responses (ABR) to click stimuli were recorded from both ears using transcutaneous silver wire electrodes placed on the top of the skull above the vertex, and directly behind the respective ear above the bullae. The stimuli were condensation clicks of 50 µs duration presented monaurally through a calibrated loudspeaker (DT 48, Beyer Dynamics, Heilbronn, GER) 100 times from 0 dB SPL p.e. to 80 dB SPL p.e. in steps of 5 dB. The signals were amplified (1000x) and filtered (0.5 kHz – 2 kHz). All subsequent signals were recorded from the pathway of the more sensitive ear (i.e. the contralateral IC). This measurement was repeated after the cochleostomy and after deafening.

2.4. Acoustic stimulation

In order to confirm correct placement along the central nucleus of the IC, and to determine the spread of excitation for a given CI electrode in the frequency space, pure tone frequency tuning curves were recorded along the IC array prior to any electrical stimulation. All acoustic stimuli were generated at 1 MHz sampling rate in AudiologyLab (Otoconsult, Frankfurt a.M., GER), and presented via a calibrated loudspeaker (DT 48). Frequency mapping of the IC was performed with 10 ms pure tones (2 ms cosine ramp) from 2 kHz to 32 kHz in steps of quarter octaves, presented at 0 dB SPL to 80 dB SPL in steps of 5 dB. Each stimulus was presented 20 times with an interstimulus interval of 37 ms.

2.5. Electrical stimulation

All electrical stimuli were generated in MATLAB (MathWorks, Natick, MA) at 100 kHz sampling rate and presented via an optically isolated constant current source (CS2, Otoconsult, Frankfurt a.M., GER) through the CI. A summary of electrical stimuli is given in Fig. 1. All electrical pulses were cathodic-leading pulses, commonly considered to be more effective in guinea pig CI stimulation (Macherey and Cazals, 2016), and were delivered in monopolar configuration. Standard biphasic stimuli were rectangular, had phase durations of 50 µs per phase, and no interphase gap (biphasic pulse, amplitude-based coding, BPA, Fig. 1a). Pseudomonophasic stimuli consisted of a first phase of 50 µs duration, no interphase gap, and a second phase of 250 µs duration (with an amplitude relation of 1:5 to the first phase). For an increase in stimulus intensity, biphasic pulses were always increased in amplitude while keeping the phase duration constant. PS were either scaled the same way (pseudomonophasic pulse, amplitude-based coding, PSA, Fig. 1c), or they were scaled by changing the phase durations (pseudomonophasic pulse, duration-based coding, PSD, Fig. 1b) while keeping the amplitudes constant, resulting in 1/5 of the current over 5 times the duration for the second phase,

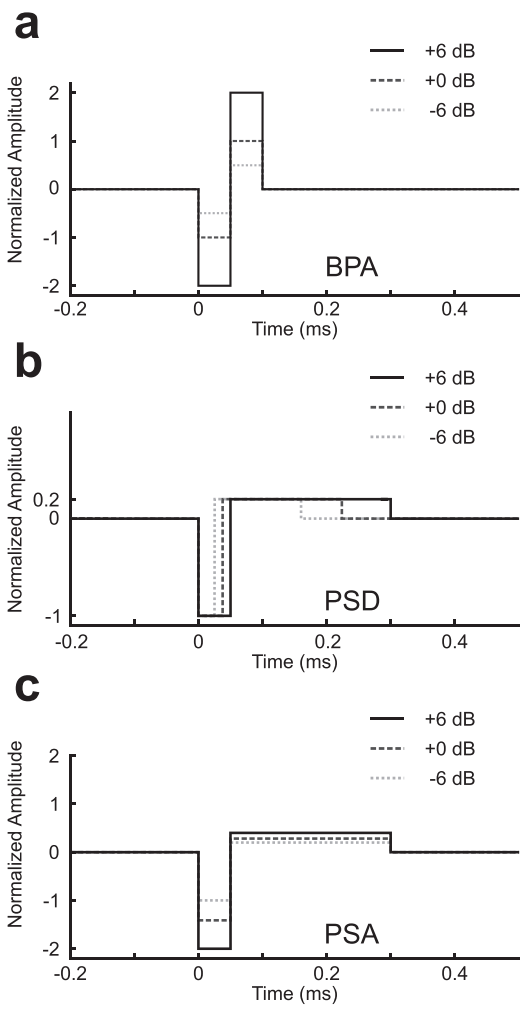

Fig. 1. Schematics of pulse shape and intensity coding combinations used in this study. a – Biphasic, amplitude-coded pulses (BPA) were used as a baseline. b, c – Pseudomonophasic, duration-coded pulses (PSD, b) and pseudomonophasic, amplitude-coded pulses (PSA, c) were used as the experimental condition stimulus.

thus carrying the same total charge (Table 1). Intensity values are thus comparable between conditions and expressed in dB of total charge relative to 500 nC, or in dB relative to threshold charge. To determine the response threshold, biphasic pulses were presented at decreasing attenuation (in steps of 1 dB) from -50 dB (corresponding to a peak current of 31.62 µA and a charge per phase of 1.58 nC) to -15 dB (corresponding to a peak current of 1.77 mA and a charge per phase of 88.91 nC). For reasons of time, we could not measure all conditions in every animal. In 12 animals, we stimulated with BPA and PSD across all paradigms. In 6 animals, we stimulated with BPA and PSA for the spread of excitation, dynamic range, and threshold measurements, and PSD and PSA for the channel interactions measurement. Two animals were used in both groups.

2.6. Single pulses

With acoustic recordings completed and the CI in place, electrical mapping was performed by presenting BPA via electrodes 2 (located towards the cochlear apex, "apical electrode") and 5 (located towards the cochlear base, "basal electrode", Fig. 2a, b). After determining the lowest threshold among the IC recording channels online, PS were presented from -6 dB to +6 dB relative to the lowest recorded threshold in 1 dB steps. These measurements were

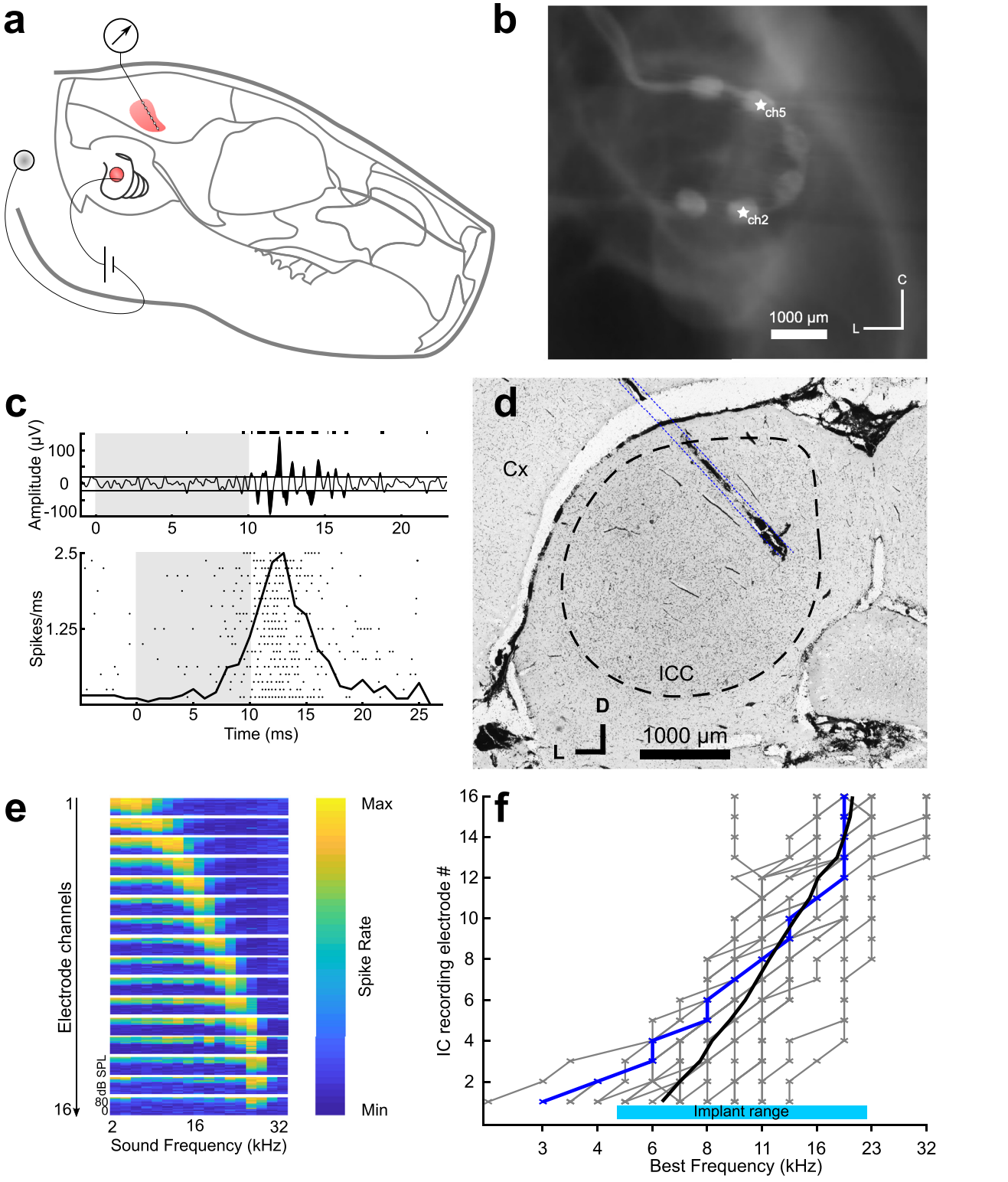

Fig. 2. a – Schematic of the recording and stimulation setup. b – Maximum projection of µCT slice images for the implanted cochlea of a single animal. Stars indicate the electrodes on the CI used for stimulation. c – Top: Example filtered recording trace (300 Hz – 3000 Hz) with spike threshold lines. The filled-in areas are suprathreshold signal parts. The bars at the top depict the detection of "spikes" in the signal. Bottom: Example raster plot with PSTH averaged over 20 trials. The grey bar indicates the acoustic stimulus. d – Cytochrome-C-oxidase staining of a post-experiment brain slice. The electrode was coated with DiI to visualize the electrode track (blue outline). e – Example recording of frequency tuning curves along the IC array from dorsal to ventral for 0 – 20 dB SPL and 2 – 32 kHz (blue curve). f – Best frequency sampling from the IC for each experiment. Solid gray lines are individual animals; the black line indicates the mean.

Table 1
All stimuli carried the same charge at the same intensity. The table shows the current intensity for the reference BPA (column 1), the reference attenuation relative to the lowest BPA threshold (column 2, 30 dB in this example), and the charge transmitted per phase (columns 3 and 4). The columns headlined by pulse shape show the current (I_p) and duration (d_p) for the first and second phase.

Attenuation (dB re 500 nC)	Attenuation (dB re THR)	Charge of phase 1 (nC)	Charge of phase 2 (nC)	BPA		PSD				PSA			
				I_p (µA)	d_p (µs)	I_{p1} (µA)	I_{p2} (µA)	d_{p1} (µs)	d_{p2} (µs)	I_{p1} (µA)	I_{p2} (µA)	d_{p1} (µs)	d_{p2} (µs)
-36	-6	7,9	7,9	158,5	50	316,2	63,2	25,1	125,3	158,5	31,7	50	250
-35	-5	8,9	8,9	177,8	50	316,2	63,2	28,1	140,6	177,8	35,6	50	250
-34	-4	10,0	10,0	199,5	50	316,2	63,2	31,5	157,7	199,5	39,9	50	250
-33	-3	11,2	11,2	223,9	50	316,2	63,2	35,4	177,0	223,9	44,8	50	250
-32	-2	12,6	12,6	251,2	50	316,2	63,2	39,7	198,6	251,2	50,2	50	250
-31	-1	14,1	14,1	281,8	50	316,2	63,2	44,6	222,8	281,8	56,4	50	250
-30	0	15,8	15,8	316,2	50	316,2	63,2	50,0	250,0	316,2	63,2	50	250
-29	1	17,7	17,7	354,8	50	316,2	63,2	56,1	280,5	354,8	71,0	50	250
-28	2	19,9	19,9	398,1	50	316,2	63,2	62,9	314,7	398,1	79,6	50	250
-27	3	22,3	22,3	446,7	50	316,2	63,2	70,6	353,1	446,7	89,3	50	250
-26	4	25,1	25,1	501,2	50	316,2	63,2	79,2	396,2	501,2	100,2	50	250
-25	5	28,1	28,1	562,3	50	316,2	63,2	88,9	444,6	562,3	112,5	50	250
-24	6	31,5	31,5	631,0	50	316,2	63,2	99,8	498,8	631,0	126,2	50	250

used to compare the response thresholds, dynamic ranges, and the spread of excitation ("overlap").

2.7. Pulse trains

After single pulse mapping, 800 ms pulse trains composed of BPA, PSA, or PSD were presented at -6 dB, 0 dB, and +6 dB relative to the lowest BPA threshold along all IC recording channels. Pulse trains were presented either in an isolated condition with only one train at one electrode (2 or 5), or a simultaneous condition with two pulse trains at two electrodes (2 and 5). In both conditions, electrode 2 (apical) always carried a 19 Hz train, while electrode 5 (basal) always carried a 37 Hz train. The pulse shape and intensity coding were always the same for both stimuli when presented simultaneously. Since none except the very first electrical pulses were overlapping, computing the stimulus locking for the individual pulse train frequencies can be used as an indirect measure for channel interactions.

2.8. Recording

All signals from the IC were recorded with a 2 × 16 Ir/IrOx electrode array with 177 µm² contacts spaced 100 µm longitudinally, and 500 µm laterally (Fig. 2a, d, NeuroNexus Technologies, Ann Arbor, MI, initial impedance ca. 100 kΩ). Signals were amplified (Neuralynx Cheetah 64-channel amplifier, 8000x, Neuralynx, Bozeman, MT), bandpass-filtered at 0.1 Hz – 9 kHz, digitized (NI-6259, National Instruments, Austin, TX) at a sampling rate of 20 kHz, and stored using AudiologyLab. As a reference electrode, a small silver ball electrode was placed epidurally directly posterior to Bregma. All signals were further processed using MATLAB.

2.9. Data analysis

All data analysis procedures were performed using custom-written MATLAB routines. Electrical artefacts were removed through linear interpolation. All individual signals were digitally bandpass-filtered at 300 Hz – 3000 Hz (0-phase delay, 4th-order Butterworth) to extract spiking activity. Spikes were extracted as described by Quiroga et al. (2004). In brief, spikes were detected when the signal amplitude exceeded three times the median signal amplitude divided by 0.6745. Since the recorded activity was multi-unit activity (MUA), a detection limit of 4 spikes per ms was set. MUA was then binned into 1 ms bins to obtain peri-stimulus time histograms, and the evoked spike rate was calculated from a 25 ms post-stimulus window. These MUA spiking responses were used to extract the best frequency (BF) of each recording channel by collapsing the responses in the intensity domain and choosing the frequency that elicited the strongest cumulative response, thus taking both response strength as well as threshold into account. The dynamic range was evaluated by fitting a four-parameter logistic equation to the firing rate/intensity level functions. The dynamic range was defined as the range from 10% – 90% of the maximal response strength. Only responses where a sufficient fit for the dynamic range was reached were further analyzed ($R^2 > 0.8$). The rare cases when saturation was not reached were excluded from further analysis. For current threshold analysis, a response was detected if the mean firing rate exceeded the mean pre-stimulus ongoing rate from a randomly selected 25 ms time window by 3 standard deviations.

Since amplitude coding (current level) and duration coding (current pulse duration) were used in the present experiments, we generally refer to stimulus strength as intensity, whereas this is always controlled in logarithmic steps (dB). To estimate the overlapping activation of the auditory pathway for two different stimulation electrodes, we computed the overlap of response activity along the IC electrode profile for single pulse stimulation at electrode 2 (apical) and electrode 5 (basal). For this, all channels with the same BF were averaged.

2.10. Overlap

For quantitative analysis of the spread of excitation, an *overlap* was defined as follows (Fig. 4): The response matrices were converted to binary values (1 = response/0 = no response, Fig. 4, "Binary") according to the threshold detection algorithm, and the activation profiles were compared over a range from the lowest threshold to 1 dB above this threshold by dividing the sum of all values in the matrix resulting from the logical AND operation (binary e2, binary e5, Fig. 4, "And") by the sum of the logical OR operation (binary e2, binary e5, Fig. 4, "OR"). This results in overlap values between 0 for no overlap and 1 for full overlap (i.e. identical excitation patterns). The binarization was performed after computing the response matrix for each channel and averaging channels with the same BF, effectively increasing the response threshold criterion strictness.

2.11. Vector strength

To investigate channel interactions, we presented two pulse trains at different frequencies both in isolation as well as simultaneously at electrodes 2 (19 Hz) and 5 (37 Hz) of the implant. All individual pulse artefacts were removed by linear interpolation, and spikes from the IC were detected as described above. The vector strength (VS) was calculated after Goldberg and Brown (1969):

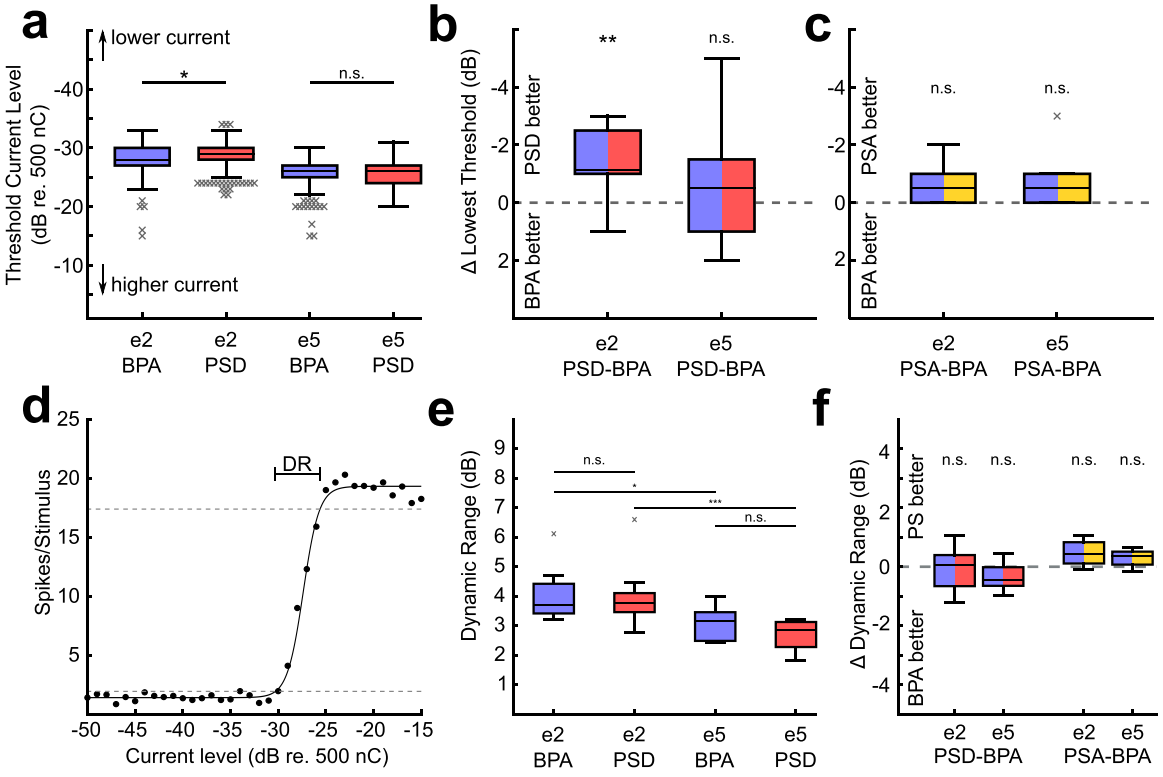

Fig. 3. a – Median IC thresholds recorded for BPA and PSD stimulation for stimulation electrodes 2 (apical) and 5 (basal). b – Difference in lowest thresholds on the IC array between BPA and PSD, grouped by stimulation electrode. A positive value indicates better thresholds for PSD stimulation. c– Same as middle for PSA. d – Dynamic range example for electrical BPA stimulation. Dashed lines indicate the 10% and 90% mark of the maximum response. The dynamic range in this case (the range between the intersections of the fit function and the 10%/90% lines) was 3.7 dB. e – There is no significant difference between the dynamic ranges for PSD and BPA stimulation, but a significant difference between stimulation electrodes 2 (apical) and 5 (basal). f – No significant effects of pulse shape or coding strategy were recorded in dependence of electrode position

Periodic pulses were treated as a periodic stimulus with a period duration corresponding to the interpulse duration. A "period" histogram was obtained by mapping the spike timings onto the interpulse periods. From such period histograms, VS were computed and statistical significance was determined by a Rayleigh-test ($\alpha = 0.05$).

2.12. Histology

In sample animals, histological analysis confirmed correct recording electrode placement in the central nucleus of the IC. The brains were extracted and fixated in 4% PFA for at least two weeks. Before staining, the brains were incubated in 30% w/v sucrose at 4 °C for 24 h before being placed in freezing medium (Neg-50, thermo scientific, Waltham, MA) and frozen at -80 °C for 4 h. After that, the brains were sliced frontally into 50 µm thick slices using a cryotome (Leica CM 3050 S, Leica Biosystems, Nussloch, Germany). All sections containing the midbrain were then mounted on glass slides and subsequently cytochrome-C-oxidase (COX) stained by incubating them in a staining solution of 52% PBS, 3% sucrose, 13% cytochrome C, and 32% diaminobenzidine (both Sigma Aldrich, St. Louis, MO) at 37°C for 4 h, and then at 4°C overnight. The slices were then examined under a phase contrast microscope (Keyence BZ-9000, Osaka, Japan).

2.13. Statistics

All statistical tests were performed using standard or custom-written MATLAB routines, with the exception of the Rayleigh test, which was performed using the Circular Statistics Toolbox (Berens, 2009). The significance levels used in this study are: n.s. ($p >= 0.05$), * ($p < 0.05$), ** ($p < 0.01$), *** ($p < 0.001$). Multiple comparisons compensation was included using the Bonferroni-Holm method. Data are presented as median + median absolute deviation (MAD). Boxplots display the median, 25th and 75th percentiles. The whiskers enclose all data points within 1.5 interquartile ranges from the 25th- and 75th percentile, respectively. All remaining points were graphically marked as individual data points, but were included in further analyses.

3. Results

Representative examples of electrode placements in the IC and the cochlea, as well as unit activity and peri-stimulus time histograms are shown in Fig. 2. Placement in the central nucleus of the IC was concluded functionally (Fig. 2c, e): MUA responses in the central nucleus are highly frequency-specific, with short latency and duration and with a progression from low to high BFs on the individual channels of the recording probe (e.g. Malmierca *et al.*, 1995). The average coverage of BFs was within the targeted CI implantation range (Fig. 2f). Histological reconstructions and COX staining further confirmed that our approach results in electrode placement in the central IC (Fig. 2d).

3.1. Thresholds

BPA, PSD and PSA were compared with respect to the unit thresholds in the IC. These thresholds varied in median between -26 and -31 dB in all stimulus configurations. However, there were subtle differences: Firstly, stimulation thresholds for the apical electrode 2 were lower than those for the basal electrode 5 (Fig. 3a; BPA: apical -28 ± 1 dB; basal -26 ± 1 dB; Wilcoxon

signed-rank test, $p < 0.001$; PSD: apical -29 ± 1 dB; basal -26 ± 2 dB; Wilcoxon signed-rank test, $p < 0.001$). Secondly, for the more sensitive electrode location (apical, electrode 2) there was also a slight but significant threshold decrease with PSD compared to BPA (Fig. 3a, difference 1 dB, Wilcoxon signed-rank test, $p = 0.046$). And finally, the difference between BPA and PSD disappeared for the more basal (less sensitive) stimulation contact 5 (Fig. 3a, difference 0 dB, Wilcoxon signed-rank test, $p = 0.702$).

Evaluating the average response threshold along the IC array can give an indication of the pulse efficiency. However, if the spread of the electric field changes from one pulse shape to the other, thresholds of units with BFs close to the stimulation site may be differently affected by the new stimulus than those further away. Therefore, we subsequently evaluated the pairwise differences in the lowest threshold along the BF-axis of the inferior colliculus for PSD to BPA (Fig. 3b) and PSA to BPA (Fig. 3c). Using the lowest threshold reduces the effect of the spread of excitation on the threshold measure. The differences were in tendency positive and significant for PSD-BPA for the apical electrode (Fig. 3b; PSD-BPA: apical -1 ± 2 dB, Wilcoxon signed-rank test, $p = 0.008$; basal -0.5 ± 2 dB, Wilcoxon signed-rank test, $p = 0.383$). For PSA-BPA, on the other hand, the differences were not significant (Fig. 3c; PSA-BPA: apical -0.5 ± 1 dB, Wilcoxon signed-rank test, $p = 0.75$; basal -0.5 ± 1 dB, Wilcoxon signed-rank test, $p = 0.25$). This demonstrates that phase duration coding reduces response thresholds, particularly at electrodes in the apical cochlea that are closer to the modiolus.

3.2. Dynamic range

The median dynamic range of the response was determined as the range between 10% and 90% of the maximum of the response strength/stimulus intensity function (Fig. 3d). The dynamic range was significantly larger for the apical electrode than for the basal electrode, corresponding to lower thresholds and the interpretation of reflecting a smaller distance to the modiolus (Fig. 3e, BPA: apical electrode 3.69 ± 0.62 dB; basal electrode 3.16 ± 0.5 dB, Wilcoxon signed-rank test, $p = 0.025$; PSD: apical electrode 3.77 ± 0.59 dB, basal electrode 2.85 ± 0.42 dB, Wilcoxon signed-rank test, $p < 0.001$). When comparing BPA to PSD for the basal- and the apical electrode, the dynamic range did not show any significant difference (Fig. 3e; Wilcoxon signed-rank test, $p = 0.998$ for apical, $p = 0.611$ for basal).

For the same reason as above, we subsequently evaluated the pairwise differences in dynamic ranges for PSD to BPA and PSA to BPA (Fig. 3f). The results did not reveal any significant differences (PSD-BPA apical 0.07 ± 0.56 dB, Wilcoxon signed-rank test, $p = 0.91$; basal -0.5 ± 0.4 dB, Wilcoxon signed-rank test, $p = 0.063$; PSA-BPA: apical 0.42 ± 0.4 dB, Wilcoxon signed-rank test, $p = 0.063$; basal 0.39 ± 0.26 dB, Wilcoxon signed-rank test, $p = 0.188$). This result demonstrates that the asymmetric pulses do not significantly influence the dynamic range.

3.3. Overlap

We compared BPA and PSD/PSA responses with regard to their functional spread of excitation by computing the overlapping activity for stimulation of electrodes 2 and 5 on the CI along the IC array. We limited this assessment only to threshold and threshold + 1 dB, since higher intensities yielded no differences in the excitation patterns (Fig. 4). The overlap was calculated as the proportion of indiscriminately responding recording channels out of all responding recording channels, thus obtaining one data point per animal (Fig. 5). For BPA, the median overlap was 0.65 ± 0.17. When presenting PSD, the median overlap was reduced by 37% down to 0.41 ± 0.1 (Fig. 5a, n = 12, Wilcoxon signed-rank test, $p = 0.007$). For PSA, there was no significant change in the overlap compared to BPA (Fig. 5b, n = 6, Wilcoxon signed-rank test, $p = 0.385$), although the data distributions showed a similar relation as in PSD in this smaller set of animals. To investigate a potential influence of pulse shape alone, we compared the difference in the group distributions of the overlap enhancement (Delta) between PSD and PSA and found no significant difference (Fig. 5c, $n = 12$ vs 6, Wilcoxon-Mann-Whitney test, $p = 0.4$). These data demonstrate a slightly reduced overlap with PSD stimuli compared to BPA at near-threshold levels.

3.4. Vector strength

To investigate the channel interactions in the temporal domain, we presented two pulse trains with different frequencies simultaneously on electrodes 2 and 5 of the CI. By evaluating the phase locking of the IC responses, we could quantify the interaction effects for the different pulse shapes. This method complemented the overlap by assessing interactions at high suprathreshold level.

To obtain a baseline, pulse trains were first presented in isolation at 6 dB above the lowest BPA response threshold recorded among all channels along the IC array (Fig. 6). 6 dB above threshold is safely in saturation of the response rate/level function (Fig. 3d). The VS values were around 0.6 for all pulse shapes and for both stimulation electrodes (Fig. 7a, Kruskal-Wallis-test, $p = 0.06$). When introducing a second stimulus on the other electrode, the grand median VS along the array dropped to values between 0.17 and 0.29 (Fig. 7b), with a few recorded units exhibiting only a small drop in VS. First, we compared how the absolute VS to one stimulus was affected by the other stimulus (19 Hz pulse train presented at the apical-, and 37 Hz at the basal electrode). The range of VS in the simultaneous condition was generally smaller with PSD stimulation compared to BPA stimulation, making the units that stayed at comparatively high VS stand out (Fig. 7b). Furthermore, the VS medians in the simultaneous condition for BPA stimuli were similar to the VS for PSD stimuli (pooled over electrodes: BPA 0.2 ± 0.18; PSD 0.21 ± 0.13, Wilcoxon signed-rank test, $p = 0.14$, data not shown in Fig. 7). However, the VS resulting from simultaneous stimulation is dependent on the VS in the isolated condition. Therefore, we expressed the VS in the simultaneous condition relative to the VS in the isolated condition, yielding a fractional value, so that no effect of the second stimulus would result in a value of 1, and a reduction of the VS would lead to a value < 1. In such a relative measure, the VS to a 19 Hz BPA train on the apical electrode was reduced by the second stimulus down to 27 ± 16% of the VS in the isolated condition. When using PSD, the VS was reduced to 32 ± 10%. Consequently, PSD reduced the VS slightly less than BPA and allowed a better channel separation (Fig. 7c, difference 4.8%, Wilcoxon signed-rank test, $p < 0.001$). For a 37 Hz BPA train presented on the basal electrode, a second stimulus reduced the VS to 49 ± 19%, while using PSD reduced the VS to 53 ± 12% (Fig. 7c, difference to BPA of 3.8%, Wilcoxon signed-rank test, $p < 0.001$). In both cases, the adverse effect of the second stimulus on the phase locking to the first stimulus was thus smaller with PSD than with BPA.

We additionally directly compared PSA to PSD in 6 animals. There was no difference between the PSA and PSD intensity coding strategies in the isolated condition (Fig. 7d, Kruskal-Wallis-test, $p = 0.767$). In the simultaneous condition, the basal and apical electrodes yielded different VS (Fig. 7e, Kruskal-Wallis test, $p<0.001$). Nonetheless, there was neither a difference between PSA and PSD for the apical electrodes (PSA 0.19 ± 0.07, PSD 0.19 ± 0.07, Wilcoxon signed-rank test, $p = 0.92$) nor for the basal elec-

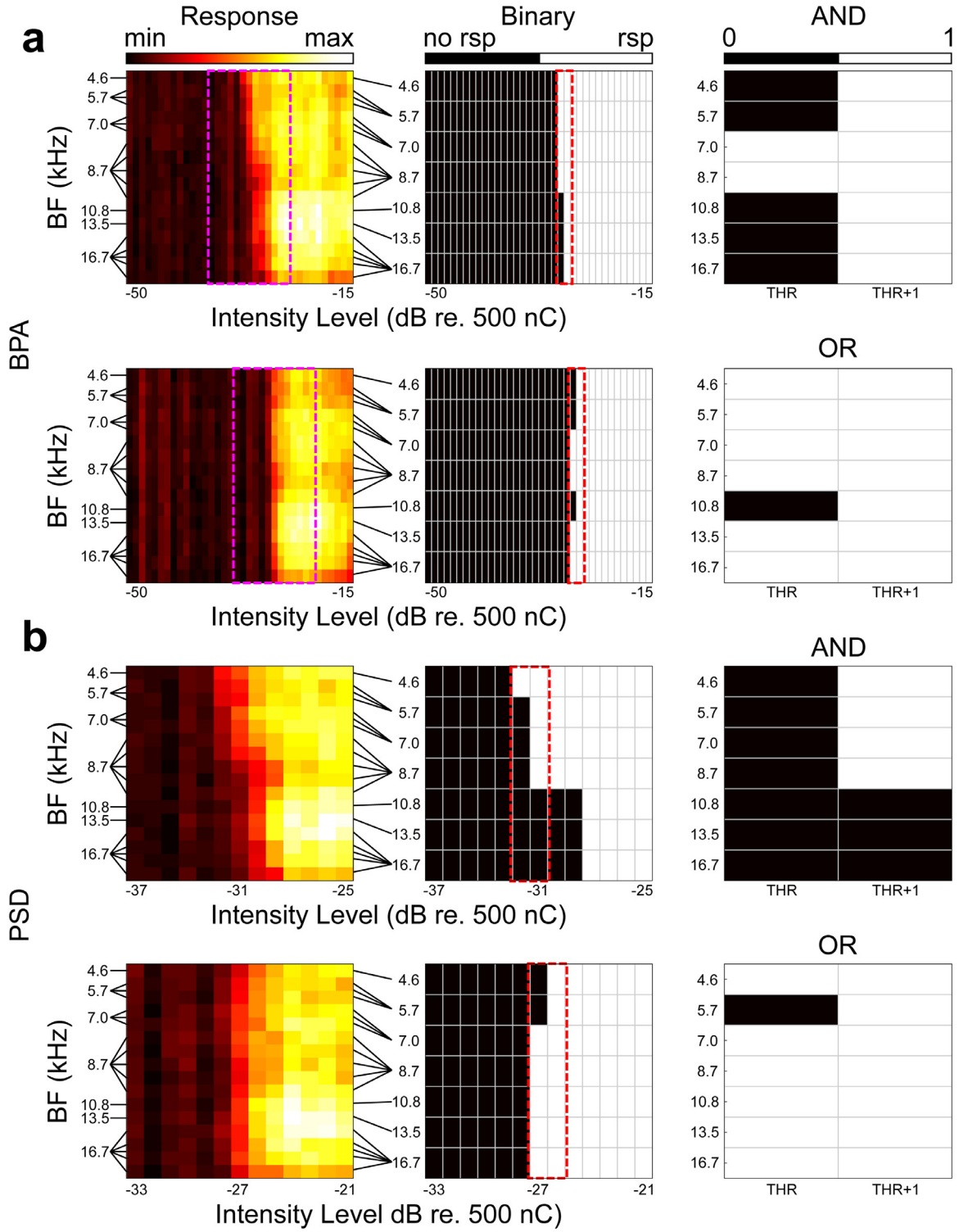

Fig. 4. Example activation profiles from a single IC position in a single animal. a – IC profiles for BPA activation for electrode 2 (top row) and electrode 5 (bottom row). The color scale ranges from the minimal to the maximal response rate for the given stimulus set and IC electrode array position across all array electrodes. The purple inset shows the range +/-6 dB around the threshold over which PSD were presented (b). Middle Column: IC profile converted to binary according to the response detection algorithm. Channels with equal BFs were averaged together before binarization to reduce any BF sampling bias. The red inset shows the range that was considered for the logical operations shown in the right column. Top Right: logical matrix for the AND operation of the highlighted areas from the two binary matrices from the middle row. Bottom Right: logical matrix for the OR operation of the highlighted areas from the two binary matrices from the middle row. b – The same for PSD pulses across the intensities shown by the purple inset.

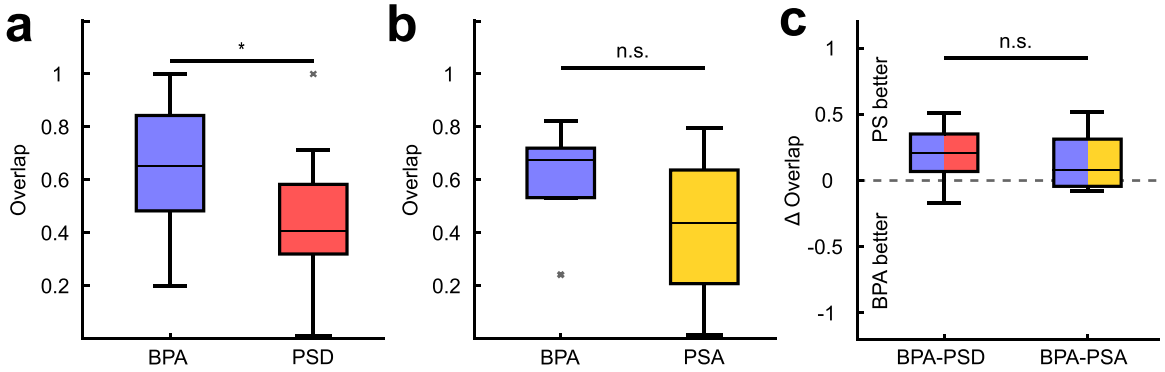

Fig. 5. a – Overlap ratio of IC activation for individual stimulation at electrodes 2 and 5 for BPA and PSD from threshold to threshold +1 dB. Statistical comparison is pair-wise. b – Same as left, but for PSA. c –There was no significant difference in the overlap enhancement between PSD or PSA.

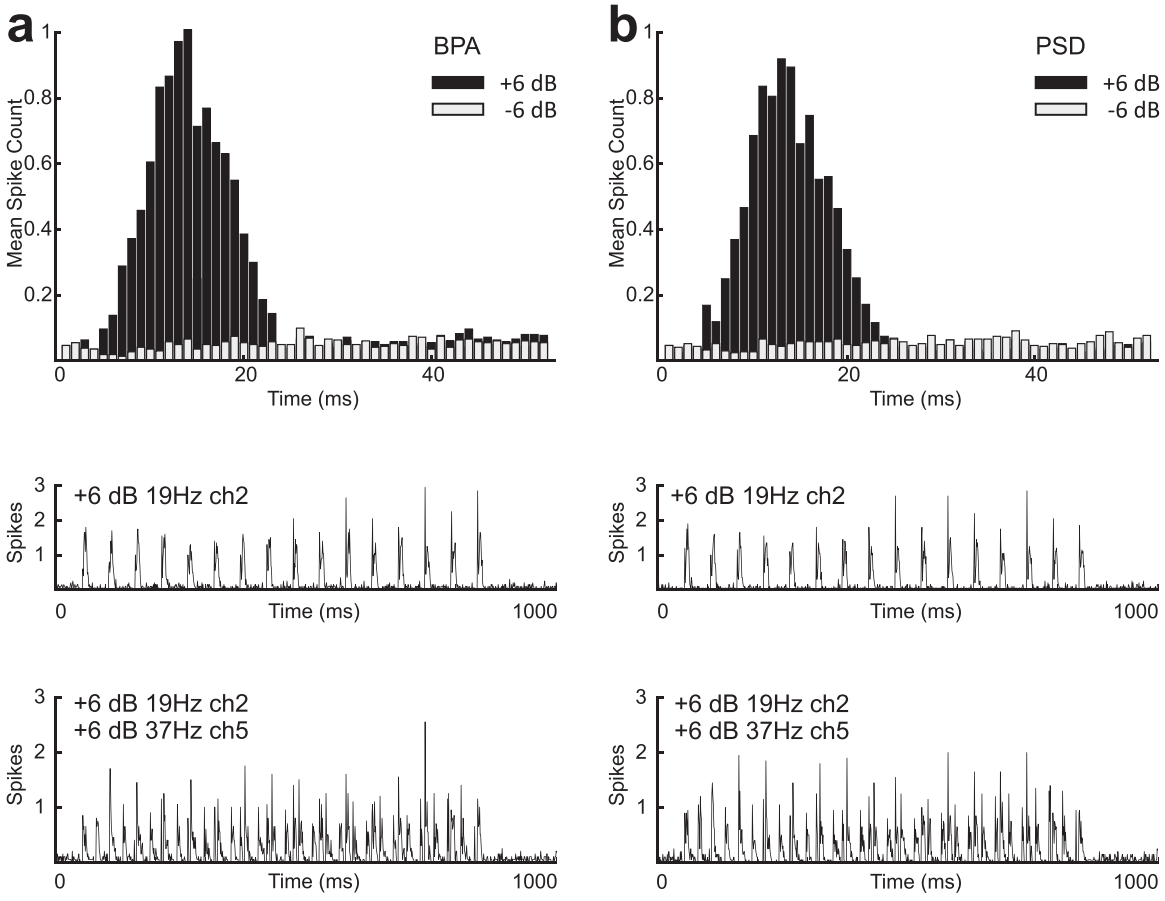

Fig. 6. a – Top to Bottom: Example of a period spike histogram for BPA stimulation. Peri-stimulus time histograms of spiking activity, averaged over 20 isolated suprathreshold presentations, and for 20 simultaneous presentations with the distracting stimulus at suprathreshold level. b – Same animal and recording position as a, but for PSD stimulation.

trodes (PSA 0.44 ± 0.10, PSD 0.45 ± 0.10, Wilcoxon signed-rank test, $p = 0.84$). Also in this case, we computed the ratio between the VS in the simultaneous and the isolated condition. There was a significantly smaller reduction of the VS for PSD presented on the apical electrode (Fig. 7f, to 29 ± 9% for PSD compared to 23 ± 6% for PSA, Wilcoxon signed-rank test, $p < 0.001$). The effect was not observed for the basal electrode, where PSD reduced the VS to 60 ± 5%, compared to 62 ± 6% for PSA (Fig. 7f, Wilcoxon signed-rank test, $p = 0.183$). Thus, the pairwise relative comparison revealed an effect of coding strategy for the apical electrodes only.

Since PSA was not different from PSD in phase locking effects in the vast majority of comparisons, but BPA and PSD were, we assume that it is mainly pulse asymmetry that positively influenced the VS both in the basal as well as the apical region. Phase duration coding had an additional effect in the apical region only, where the current spread and the distance to the target neurons are presumably smaller.

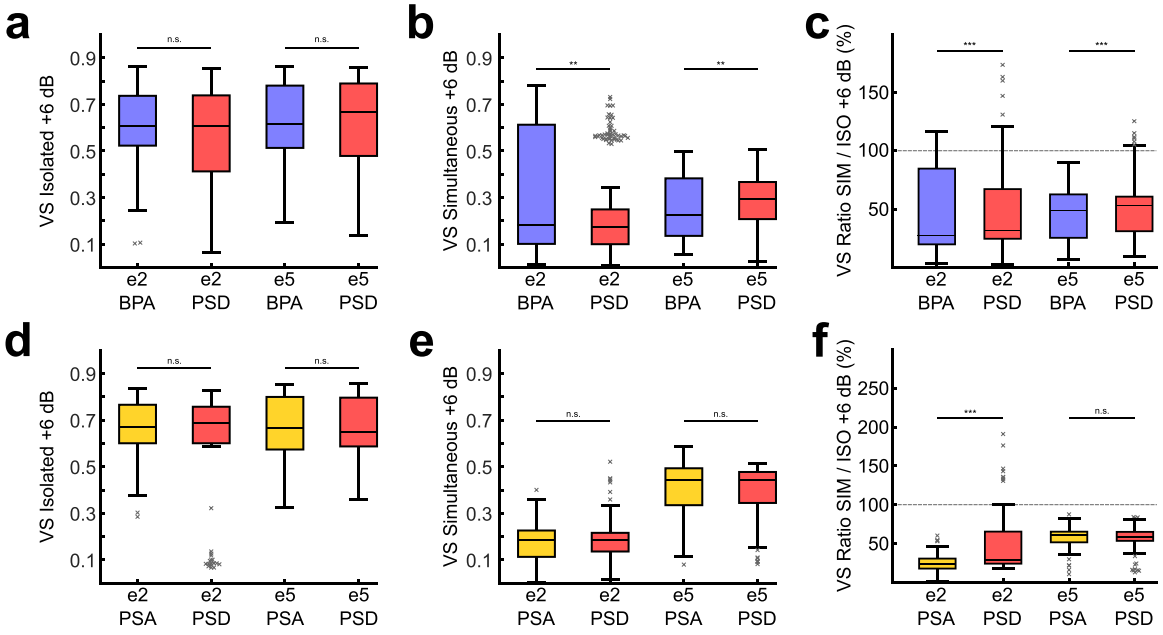

Fig. 7. a – VS for isolated presentation of a 19Hz (e2) or a 37Hz (e5) pulse train of either BPA or PSD at threshold +6 dB. b – VS for simultaneous presentation of a 19Hz (e2) and a 37Hz (e5) pulse trains of either BPA or PSD at threshold +6 dB. c – Pair-wise ratio of simultaneous VS / isolated VS. d, e, f – same as top, but comparison between PSA and PSD. All statistical comparisons include points graphically marked as outliers.

4. Discussion

In this study, we compared a phase-duration-coded pseudomonophasic CI stimulus with the standard, amplitude-coded biphasic stimulus, with respect to the spread of excitation at threshold intensities, and the channel separation at suprathreshold intensities. Electric intensity coding using phase duration with pseudomonophasic pulses provided lower thresholds, a reduced spread of excitation, as well as a decrease in channel interactions. With monopolar stimulation, a reduction of channel interactions by about 5% was achieved. This would approximately translate to an additional channel of information on a 20-channel cochlear implant.

4.1. Thresholds

The positive effects of monophasic and pseudomonophasic pulses on eCAP- and auditory nerve thresholds have been thoroughly documented (Miller et al., 2001; Shepherd and Javel, 1999). In the present study, we found lower thresholds for PS stimuli only when combined with phase duration coding, and the effect was stronger for the apical electrode. In the apical region, the scala tympani has a smaller volume, and thus the electrode is located closer to the modiolus with less shunt-current in the perilymph (Shepherd et al., 1993; Shinomori et al., 2001). This appears to be a favorable condition for PS stimulation and is most likely the reason for the basal-to-apical differences found in this study.

PSA coding was previously reported to generate lower eCAP thresholds than BPA (Miller et al., 2001), an observation that we could not replicate in the present study. This discrepancy is likely due to the ratio of the phase amplitudes (present study: 1:5, Miller et al.: 1:10). Furthermore, we investigated IC thresholds and Miller et al. investigated peripheral thresholds. Studies with cochlear implanted human subjects showed slightly enhanced threshold- and most-comfortable levels for pseudomonophasic pulses similar to ours when used in pulse trains at rates from 98 to 800 Hz (Macherey et al., 2006; Van Wieringen et al., 2005). Using pulse train stimulation, however, the threshold is also the consequence of the integration over time, which would not necessarily be reflected in single-pulse stimulation data presented here (van Wieringen et al., 2006). A systematic investigation of this effect has not been provided yet.

4.2. Dynamic range

We found no differences in the neuronal dynamic ranges achieved with BPA, PSD, or PSA stimuli. Previous eCAP measurements conducted in guinea pigs have shown no preference in grand mean data for these coding strategies, but large inter-individual variability in the eCAP growth functions (Adenis et al., 2018). We did not observe highly variable individual dynamic ranges. However, the previous study used anodic PS, as opposed to cathodic PS employed in the present study, and was conducted in chronically stimulated animals with variable residual hearing, allowing electrophonic responses that may increase the electric dynamic range substantially (Sato et al., 2016). While the majority of animals in our study showed no significant differences in dynamic range between BPA and PS, the few that did display a significant difference consistently had a smaller dynamic range for PSD compared to BPA (data not shown). Notably, compound action potential recordings are also contaminated by stimulation artifacts that might have contributed to the high variability in the previous results (Hughes et al., 2017; Klop et al., 2004).

4.3. Overlap

By demonstrating a significant overlap reduction by 37% with PSD compared to BPA, but no significant difference when comparing PSA to BPA, Fig. 5 (a, b) might suggest that duration coding is responsible for the reduced spread of excitation observed in the present study. However, when comparing the effects of PSA and PSD, it is important to acknowledge that experiments with PSA were performed with a smaller number of animals than the comparisons of PSD vs. BPA (see methods), affecting statistical sensitivity. Fig. 5 (a, b) in fact shows a similar relation of BPA to both PSA as well as PSD. We suspected that the pulse shape alone may have

the main influence on the spread of excitation. Therefore, we investigated the difference in the effects between PSD and PSA, and found a similar reduction in overlap (Fig. 5c).

The main difference between BP and PS stimuli is the omission of one polarity in the suprathreshold region. Cathodic and anodic stimuli excite axons at different locations (Ranck, 1975). Thus, biphasic stimuli may recruit two distinct (albeit largely overlapping) populations of spiral ganglion cells in very close succession, increasing the spread of excitation compared to cathodic PS stimuli. The use of monopolar pseudomonophasic stimuli was previously suggested to reduce the spread of excitation measured by psychophysical forward masking threshold patterns in humans (Macherey et al., 2010). However, the effect was observed only in 2 out of 6 tested subjects. When comparing human data to animal data, it is important to acknowledge that many biasing factors cannot be controlled in a clinical setting. One essential factor is the degeneration of spiral ganglion cells. While in humans, the residual population of spiral ganglion cells may be 30% of the normal count or less (Nadol, 1997; Nadol et al., 2001, 1989), acute pharmacological deafening in animals leaves the number of spiral ganglion cells initially unchanged (Leake-Jones et al., 1980; Leake-Jones and Vivion, 1979). A patchy degeneration, as found in clinical populations, has obvious consequences for the investigation of the effects of spread of excitation (Jahn and Arenberg, 2019b). Whether this outcome variability in human subjects is related to the specific location of the implant, a patchy degeneration of the nerve, the site of spike initiation and the degeneration of primary afferents, central auditory processing, or other aspects of stimulation, remains to be clarified in the future. To reduce these biasing factors, objective measures of spiral ganglion degeneration are needed in clinical settings to verify animal study results (Pfingst et al., 2015). Our results support the reduced spread of excitation using PS, but this would likely only be reflected in forward masking tests if spiral ganglion cell degeneration was negligible or very even along the cochlea in the tested subjects.

The observed reduced spread of excitation for PSD can be theoretically derived from Coulomb's Law of the spread of static electric fields, which states that the instantaneous electric field strength at a given point in space due to a point charge is proportional to the instantaneous charge and the distance between the points. This simplified model has previously been validated for the cochlea as an approximation (Sibella et al., 2007; Tognola et al., 2007), and it follows that the presentation of lower current amplitudes (i.e. less instantaneous charge, albeit over a longer time period, thus injecting equal amounts of total charge) leads to a spatially more confined suprathreshold electric field. This may provide the explanation for why PSD was in some cases (apically) beneficial compared to PSA. However, the quantification of the spread of excitation with the neural activation overlap method strongly depends on the intensity range considered, which is why we additionally used the vector strength as a quantitative measure.

4.4. Vector strength

To investigate the interaction between two channels stimulated at high intensities, we analyzed the extent to which the stimulus locking to one stimulus is reduced when a second stimulus is added. We hypothesized that PS stimuli may increase the fidelity and limit the channel interactions compared to BPA by reducing the spread of excitation, regardless of intensity coding. Indeed, we found a decrease in interaction between stimulation channels of about 4-5% with PS stimuli (Fig. 7c, f). Since BPA stimuli include both high cathodic and anodic peak currents, but PS stimuli do not, PS stimulation may reduce the spread of excitation by activating a smaller population of neurons with the active cathodic-only phase. PSD stimuli reduce the peak current in both phases and thus should have a more pronounced effect than PSA stimuli. We could observe this only in one specific configuration: When computed with respect to the apical stimulus in the presence of the basal stimulus, the channel interactions (reduction in VS) were mitigated more strongly for simultaneous PSD than for PSA stimuli (Fig. 7f). A possible explanation for this discrepancy along the cochlea is the higher current spread on electrode 5 due to the anatomy at the cochlear base. The distance between the electrode and the modiolus, as well as the volume around the implant, is larger in the basal- than in the apical region, which has direct adverse consequences for the efficiency of electric stimulation (Shepherd et al., 1993). Despite being presented at the same level above threshold in both regions, the higher absolute current required basally (becuase of higher thresholds) inadvertently also leads to a larger spread of excitation. As described above, the region of suprathreshold excitation is larger with higher currents, and it follows that the presentation of less maximal current, even though over a longer time period, leads to a spatially more confined suprathreshold electric field. Over long distances, however, the spread of excitation caused by the higher amplitude may conceal this effect. The VS for simultaneous stimulation was generally higher for the basal electrode 5 than for the apical electrode 2, both in absolute (Fig. 7b, e) and relative (Fig. 7c, f) measures, meaning that the phase locking to the stimulus presented on electrode 2 is more affected by the stimulus on electrode 5 than vice versa. Since it was always the 19 Hz stimulus that was presented on the apical electrode, and the 37 Hz stimulus on the basal electrode, there is a difference in the absolute number of pulses presented per stimulus on each of the electrodes. Thus, in the simultaneous condition, the VS on the apical electrode is affected by more "disturbing" pulses from the basal electrode than vice versa. This could be the reason for the generally higher VS to basal stimulation in the simultaneous condition, but it does not compromise the relative comparison. It should further be noted that a subset of units retained relatively high VS when adding the competitive stimulus (Fig. 7b). It is possible that this is a physiological/technical phenomenon resulting from asymmetric input strength – activation of electrode 2 excited the cells towards the centroid of the electric field, while stimulation through electrode 5 excited the cells less reliably at the edge of the electric field. In this case, there would be overlapping activation in single pulse stimulation that would not necessarily be reflected in simultaneous stimulation.

There are some confounding factors that need to be considered: Firstly, it should be noted that the VS is a temporal precision measure. Changing the phase duration has implications for the temporal integration of the stimulus, and an increasing it could lead to more jitter and thus a lower VS, i.e. an adverse effect of duration coding. However, our data document no such effect for isolated stimulation. For simultaneous stimulation, we found the opposite in the apical region, and no change in the basal region. This adverse effect may nonetheless be present and only manifest in the basal region, where the current spread is so wide that a possible increase in jitter cannot be mitigated anymore by a decrease in the spread of excitation. Secondly, the thresholds are also of importance for the VS evaluation. Given that BPA are presented at a higher current level (due to higher thresholds), the convergence within the auditory system might lead to a stronger synchronization with the stimulus. The enhanced fidelity recorded here could thus be a consequence of the lower suprathreshold levels for PS stimuli compared to BPA stimuli. However, we accounted for this by keeping the current level well within the saturation of the dynamic range at threshold +6 dB, around 3 dB above the median dynamic range. Further, the VS is normalized to the total number of spikes, meaning that the result cannot be based on a mere

increased spike rate. Using intensity levels in the saturation of the response thus excludes the influence of the slightly different thresholds. Consistent with the above considerations, we propose two effects that can explain the findings – a pulse shape effect that is likely related to polarity and the excited neuronal populations, and an intensity coding effect that is likely mediated by the spread of the electric field itself.

4.5. Clinical application

The present experiments were performed on preserved spiral ganglia to avoid the biasing factor of differences in neural "health". While this is an advantage for the present experiments, it may constitute a factor to consider when translating the outcomes to human CI subjects, where neural health varies considerably. Likewise, a potential drawback of the phase-duration-based intensity coding in a CI sound processing strategy is the longer stimulus and thus the necessity of a reduced stimulation rate. Depending on the dynamic range, the maximum pulse rate for such a strategy using the phase durations tested here would cap around 1500 pps (+6 dB) to 2500 pps (+3 dB). In the best-case scenario, an increase in information transmission fidelity of 5% per channel, as it was found here, would add up to one additional channel of information on a 20-channel implant, provided that there are no redundant channels. However, this increase was determined from interactions between electrodes 2 and 5, and not neighboring electrodes.

It is likely that the present outcomes are affected by electrode spacing, which should be a focus of follow-up experiments. We expect that the benefit may become more apparent with more closely spaced electrodes. However, a closer spacing might also increase the channel interactions so much that the sensitivity of this method of investigation will be too low to show any potential advantage. There is limited evidence suggesting that in monopolar configuration, the electrode spacing influences the degree of channel interactions, but not necessarily to the degree that might be expected (Stickney et al, 2006), warranting further investigation in this direction.

Finally, it is difficult to quantify or even estimate the exact impact on speech understanding of 5% less channel interactions, because an additional electrode does not equal an additional channel of information. Vocoder studies have more or less successfully tried to compare the number of electrodes on a CI to spectral bands (Başkent, 2006; Friesen et al., 2001). If an additional channel of information for a CI-user is indeed similar to an additional spectral vocoder band, significantly improved speech understanding could be possible. Encouragingly, it has previously been shown that the positive effect of reduced channel interactions on speech understanding is stronger, the fewer channels are available to begin with (Bingabr et al., 2008).

5. Conclusions

The present results suggest that pseudomonophasic stimuli may reduce the spread of excitation, with duration coding holding an additional advantage over amplitude coding. This kind of stimulation could provide approximately one additional channel of information to present day cochlear implants. Using PS stimuli in more confined, multipolar configurations could prove even more effective, especially in combination with phase duration-based intensity coding. It would therefore be worthwhile to test this configuration in forward masking-, pitch ranking-, and speech perception studies involving human patients to confirm the beneficial effects in clinical practice.

Declaration of Competing Interest

Research CIs were supplied by Oticon medical. Authors DG and PS are employees of Oticon medical. All other authors have nothing to declare.

CRediT authorship contribution statement

Gunnar Lennart Quass: Conceptualization, Methodology, Software, Formal analysis, Investigation, Writing - original draft, Writing - review & editing, Visualization. **Peter Baumhoff:** Conceptualization, Methodology, Investigation, Writing - review & editing. **Dan Gnansia:** Conceptualization, Writing - review & editing. **Pierre Stahl:** Conceptualization, Writing - review & editing. **Andrej Kral:** Conceptualization, Writing - review & editing, Funding acquisition, Supervision.

Acknowledgements

The present study was supported by the William Demant Foundation and Deutsche Forschungsgemeinschaft (Exc 2177). The authors wish to thank Karl-Jürgen Kühne and Daniela Kühne for help with the histology and for technical assistance, and the anonymous reviewers for their helpful comments.

References

Adenis, V., Gourévitch, B., Mamelle, E., Recugnat, M., Stahl, P., Gnansia, D., Nguyen, Y., Edeline, J.-M., 2018. ECAP growth function to increasing pulse amplitude or pulse duration demonstrates large inter-animal variability that is reflected in auditory cortex of the guinea pig. PLoS One 13, e0201771. doi:10.1371/journal.pone.0201771.

Azadpour, M., McKay, C.M., Svirsky, M.A., 2018. Effect of pulse rate on loudness discrimination in cochlear implant users. JARO - J. Assoc. Res. Otolaryngol. 19, 287–299. doi:10.1007/s10162-018-0658-8.

Baskent, D., 2006. Speech recognition in normal hearing and sensorineural hearing loss as a function of the number of spectral channels. J. Acoust. Soc. Am. 120, 2908–2925. doi:10.1121/1.2354017.

Berens, P., 2009. CircStat : a MATLAB toolbox for circular statistics. J. Stat. Softw. 31, 293–295. doi:10.18637/jss.v031.i10.

Berg, K.A., Noble, J.H., Dawant, B.M., Dwyer, R.T., Labadie, R.F., Gifford, R.H., 2019. Speech recognition as a function of the number of channels in perimodiolar electrode recipients. J. Acoust. Soc. Am. 145, 1556–1564. doi:10.1121/1.5092350.

Bierer, J.A., 2007. Threshold and channel interaction in cochlear implant users: Evaluation of the tripolar electrode configuration. J. Acoust. Soc. Am. 121, 1642–1653. doi:10.1121/1.2436712.

Bierer, J.A., Middlebrooks, J.C., 2002. Auditory cortical images of cochlear-implant stimuli: dependence on electrode configuration. J. Neurophysiol. 87, 478–492. doi:10.1152/jn.00212.2001.

Bingabr, M., Espinoza-Varas, B., Loizou, P.C., 2008. Simulating the effect of spread of excitation in cochlear implants. Hear. Res. 241, 73–79. doi:10.1016/j.heares.2008.04.012.

Boulet, J., White, M., Bruce, I.C., 2016. Temporal considerations for stimulating spiral ganglion neurons with cochlear implants. JARO - J. Assoc. Res. Otolaryngol. 17, 1–17. doi:10.1007/s10162-015-0545-5.

Busby, P.A., Clark, G.M., 1997. Pitch and loudness estimation for single and multiple pulse per period electric pulse rates by cochlear implant patients. J. Acoust. Soc. Am. 101, 1687–1695. doi:10.1121/1.418178.

Carlyon, R.P., Deeks, J.M., Undurraga, J., Macherey, O., van Wieringen, A., 2017. Spatial selectivity in cochlear implants: effects of asymmetric waveforms and development of a single-point measure. JARO - J. Assoc. Res. Otolaryngol. 18, 711–727. doi:10.1007/s10162-017-0625-9.

Chatterjee, M., Fu, Q.-J., Shannon, R.V., 2000. Effects of phase duration and electrode separation on loudness growth in cochlear implant listeners. J. Acoust. Soc. Am. 107, 1637–1644. doi:10.1121/1.428448.

Dorman, M.F., Loizou, P.C., Rainey, D., 1997. Speech intelligibility as a function of the number of channels of stimulation for signal processors using sine-wave and noise-band outputs. J. Acoust. Soc. Am. 102, 2403–2411. doi:10.1121/1.419603.

Fishman, K.E., Shannon, R.V., Slattery, W.H., 1997. Speech recognition as a function of the number of electrodes used in the SPEAK cochlear implant speech processor. J. Speech, Lang. Hear. Res. 40, 1201–1215. doi:10.1044/jslhr.4005.1201.

Friedmann, D.R., Kamen, E., Choudhury, B., Roland, J.T., 2019. Surgical experience and early outcomes with a slim perimodiolar electrode. Otol. Neurotol. 40, e304–e310. doi:10.1097/MAO.0000000000002129.

Friesen, L.M., Shannon, R.V., Baskent, D., Wang, X., 2001. Speech recognition in noise as a function of the number of spectral channels: comparison of acoustic hearing and cochlear implants. J. Acoust. Soc. Am. 110, 1150–1163. doi:10.1121/1.1381538.

Goldberg, J.M., Brown, P.B., 1969. Response of binaural neurons of dog superior olivary complex to dichotic tonal stimuli: some physiological mechanisms of sound localization. J. Neurophysiol. 32, 613–636. doi:10.1152/jn.1969.32.4.613.

Hughes, M.L., Goehring, J.L., Baudhuin, J.L., 2017. Effects of stimulus polarity and artifact reduction method on the electrically evoked compound action potential. Ear Hear 38, 332–343. doi:10.1097/AUD.0000000000000392.

Jahn, K.N., Arenberg, J.G., 2019a. Polarity sensitivity in pediatric and adult cochlear implant listeners. Trends Hear 23, 1–22. doi:10.1177/2331216519862987.

Jahn, K.N., Arenberg, J.G., 2019b. Evaluating psychophysical polarity sensitivity as an indirect estimate of neural status in cochlear implant listeners. JARO - J. Assoc. Res. Otolaryngol. 20, 415–430. doi:10.1007/s10162-019-00718-2.

Kileny, P.R., Zimmerman-Phillips, S., Zwolan, T.A., Kemink, J.L., 1992. Effects of channel number and place of stimulation on performance with the cochlear corporation multichannel implant. Am. J. Otol 13, 117–123.

Klop, W.M.C., Hartlooper, A., Briare, J.J., Frijns, J.H.M., 2004. A new method for dealing with the stimulus artefact in electrically evoked compound action potential measurements. Acta Otolaryngol 124, 137–143. doi:10.1080/00016480310016901.

Kral, A., Hartmann, R., Mortazavi, D., Klinke, R., 1998. Spatial resolution of cochlear implants: The electrical field and excitation of auditory afferents. Hear. Res. 121, 11–28. doi:10.1016/S0378-5955(98)00061-6.

Leake-Jones, P.A., O'Reilly, B.F., Vivion, M.C., 1980. Neomycin ototoxicity: ultrastructural surface pathology of the organ of Corti. Scan. Electron Microsc 427–434.

Leake-Jones, P.A., Vivion, M.C., 1979. Cochlear pathology in cats following administration of neomycin sulfate. Scan. Electron Microsc 983–991.

Macherey, O., Carlyon, R.P., Van Wieringen, A., Deeks, J.M., Wouters, J., 2008. Higher sensitivity of human auditory nerve fibers to positive electrical currents. JARO - J. Assoc. Res. Otolaryngol. 9, 241–251. doi:10.1007/s10162-008-0112-4.

Macherey, O., Cazals, Y., 2016. Effects of pulse shape and polarity on sensitivity to cochlear implant stimulation: a chronic study in guinea pigs. In: van Dijk, P., Baskent, D., Gaudrain, E., de Kleine, E., Wagner, A., Lanting, C. (Eds.), Physiology, Psychoacoustics and Cognition in Normal and Impaired Hearing. Springer International Publishing, Cham, pp. 133–142. doi:10.1007/978-3-319-25474-6_15.

Macherey, O., Van Wieringen, A., Carlyon, R.P., Deeks, J.M., Wouters, J., 2006. Asymmetric pulses in cochlear implants: effects of pulse shape, polarity, and rate. JARO - J. Assoc. Res. Otolaryngol. 7, 253–266. doi:10.1007/s10162-006-0040-0.

Macherey, O., van Wieringen, A., Carlyon, R.P., Dhooge, I., Wouters, J., 2010. Forward-masking patterns produced by symmetric and asymmetric pulse shapes in electric hearing. J. Acoust. Soc. Am. 127, 326–338. doi:10.1121/1.3257231.

Malmierca, M.S., Rees, A., Le Beau, F.E.N., Bjaalie, J.G., 1995. Laminar organization of frequency-defined local axons within and between the inferior colliculi of the guinea pig. J. Comp. Neurol. 357, 124–144. doi:10.1002/cne.903570112.

Miller, C.A., Robinson, B.K., Rubinstein, J.T., Abbas, P.J., Runge-Samuelson, C.L., 2001. Auditory nerve responses to monophasic and biphasic electric stimuli. Hear. Res. 151, 79–94. doi:10.1016/S0300-2977(00)00082-6.

Nadol, J.B., 1997. Patterns of neural degeneration in the human cochlea and auditory nerve: Implications for cochlear implantation. Otolaryngol. - Head Neck Surg. 117, 220–228. doi:10.1016/S0194-5998(97)70178-5.

Nadol, J.B., Burgess, B.J., Gantz, B.J., Coker, N.J., Ketten, D.R., Kos, I., Roland, J.T., Shiao, J.Y., Eddington, D.K., Montandon, P., Shallop, J.K., 2001. Histopathology of cochlear implants in humans. Ann. Otol. Rhinol. Laryngol. 110, 883–891. doi:10.1177/000348940111000914.

Nadol, J.B., Young, Y.-S., Glynn, R.J., 1989. Survival of spiral ganglion cells in profound sensorineural hearing loss: implications for cochlear implantation. Ann. Otol. Rhinol. Laryngol. 98, 411–416. doi:10.1177/000348948909800602.

Parkins, C.W., Colombo, J., 1987. Auditory-nerve single-neuron thresholds to electrical stimulation from scala tympani electrodes. Hear. Res. 31, 267–285. doi:10.1016/0378-5955(87)90196-1.

Pfingst, B.E., De Haan, D.R., Holloway, L.a., 1991. Stimulus features affecting psychophysical detection thresholds for electrical stimulation of the cochlea. I: Phase duration and stimulus duration. J. Acoust. Soc. Am. 90, 1857–1866. doi:10.1121/1.401665.

Pfingst, B.E., Holloway, L.A., Zwolan, T.A., Collins, L.M., 1999. Effects of stimulus level on electrode-place discrimination in human subjects with cochlear implants. Hear. Res. 134, 105–115. doi:10.1016/S0378-5955(99)00079-9.

Pfingst, B.E., Zhou, N., Colesa, D.J., Watts, M.M., Strahl, S.B., Garadat, S.N., Schvartz-Leyzac, K.C., Budenz, C.L., Raphael, Y., Zwolan, T.A., 2015. Importance of cochlear health for implant function. Hear. Res. 322, 77–88. doi:10.1016/j.heares.2014.09.009.

Quiroga, R.Q., Nadasdy, Z., Ben-Shaul, Y., 2004. Unsupervised spike detection and sorting with wavelets and superparamagnetic clustering. Neural Comput 16, 1661–1687. doi:10.1162/089976604774201631.

Ranck, J.B., 1975. Which elements are excited in electrical stimulation of mammalian central nervous system: a review. Brain Res 98, 417–440. doi:10.1016/0006-8993(75)90364-9.

Rattay, F., 1986. Analysis of models for external stimulation of axons. Ieee Trans. Biomed. Eng. 33, 974–977.

Resnick, J.M., O'Brien, G.E., Rubinstein, J.T., 2018. Simulated auditory nerve axon demyelination alters sensitivity and response timing to extracellular stimulation. Hear Res 361, 121–137. doi:10.1016/j.heares.2018.01.014.

Sato, M., Baumhoff, P., Kral, A., 2016. Cochlear Implant stimulation of a hearing ear generates separate electrophonic and electroneural responses. J. Neurosci. 36, 54–64. doi:10.1523/JNEUROSCI.2968-15.2016.

Shannon, R.V., 1985. Threshold and loudness functions for pulsatile stimulation of cochlear implants. Hear. Res. 18, 135–143. doi:10.1016/0378-5955(85)90005-X.

Shepherd, R.K., Hatsushika, S., Clark, G.M., 1993. Electrical stimulation of the auditory nerve: The effect of electrode position on neural excitation. Hear. Res. 66, 108–120. doi:10.1016/0378-5955(93)90265-3.

Shepherd, R.K., Javel, E., 1999. Electrical stimulation of the auditory nerve: II. effect of stimulus waveshape on single fibre response properties. Hear. Res. 130, 171–188. doi:10.1016/S0378-5955(99)00011-8.

Shinomori, Y., Jones, D.D., Spack, D.S., Kimura, R.S., 2001. Volumetric and dimensional analysis of the guinea pig inner ear. Ann. Otol. Rhinol. Laryngol. 110, 91–98. doi:10.1177/000348940111000117.

Sibella, F., Parazzini, M., Pesatori, A., Paglialonga, A., Norgia, M., Ravazzani, P., Tognola, G., 2007. Modeling and computation of electric potential field distribution generated in cochlear tissues by cochlear implant stimulations. In: 2007 3rd International IEEE/EMBS Conference on Neural Engineering. IEEE, pp. 506–509. doi:10.1109/CNE.2007.369720.

Stickney, G.S., Loizou, P.C., Mishra, L.N., Assmann, P.F., Shannon, R.V., Opie, J.M., 2006. Effects of electrode design and configuration on channel interactions. Hear. Res. 211, 33–45. doi:10.1016/j.heares.2005.08.008.

ter Keurs, M., Festen, J.M., Plomp, R., 1992. Effect of spectral envelope smearing on speech reception. I.. J. Acoust. Soc. Am. 91, 2872–2880. doi:10.1121/1.402950.

Tognola, G., Pesatori, A., Norgia, M., Parazzini, M., Di Rienzo, L., Ravazzani, P., Burdo, S., Grandori, F., Svelto, C., 2007. Numerical modeling and experimental measurements of the electric potential generated by cochlear implants in physiological tissues. IEEE Trans. Instrum. Meas. 56, 187–193. doi:10.1109/TIM.2006.887334.

Traunmüller, H., 1990. Analytical expressions for the tonotopic sensory scale. J. Acoust. Soc. Am. 88, 97–100. doi:10.1121/1.399849.

Undurraga, J.A., Carlyon, R.P., Macherey, O., Wouters, J., van Wieringen, A., 2012. Spread of excitation varies for different electrical pulse shapes and stimulation modes in cochlear implants. Hear. Res. 290, 21–36. doi:10.1016/j.heares.2012.05.003.

Undurraga, J.A., Carlyon, R.P., Wouters, J., Van Wieringen, A., 2013. The polarity sensitivity of the electrically stimulated human auditory nerve measured at the level of the brainstem. JARO - J. Assoc. Res. Otolaryngol. 14, 359–377. doi:10.1007/s10162-013-0377-0.

van den Honert, C., Kelsall, D.C., 2007. Focused intracochlear electric stimulation with phased array channels. J. Acoust. Soc. Am. 121, 3703–3716. doi:10.1121/1.2722047.

Van Wieringen, A., Carlyon, R.P., Laneau, J., Wouters, J., 2005. Effects of waveform shape on human sensitivity to electrical stimulation of the inner ear. Hear. Res. 200, 73–86. doi:10.1016/j.heares.2004.08.006.

van Wieringen, A., Carlyon, R.P., Macherey, O., Wouters, J., 2006. Effects of pulse rate on thresholds and loudness of biphasic and alternating monophasic pulse trains in electrical hearing. Hear. Res. 220, 49–60. doi:10.1016/j.heares.2006.06.015.

van Wieringen, A., Macherey, O., Carlyon, R.P., Deeks, J.M., Wouters, J., 2008. Alternative pulse shapes in electrical hearing. Hear. Res. 242, 154–163. doi:10.1016/j.heares.2008.03.005.

Zhou, N., Xu, L., Pfingst, B.E., 2012. Characteristics of detection thresholds and maximum comfortable loudness levels as a function of pulse rate in human cochlear implant users. Hear. Res. 284, 25–32. doi:10.1016/J.HEARES.2011.12.008.

Zwicker, E., Fastl, H., 1999. Psychoacoustics, Springer Series in Information Sciences. Springer Berlin Heidelberg, Berlin, Heidelberg doi:10.1007/978-3-662-09562-1.

Zwicker, E., Flottorp, G., Stevens, S.S., 1957. Critical band width in loudness summation. J. Acoust. Soc. Am. 29, 548–557. doi:10.1121/1.1908963.